Article

Linear Radical Additions-Coupling Polymerization (LRAsCP): Model, Experiment and Application

Yudian Jiang [1] , **Kun Cao** [2] **and Qi Wang** [1,*]

1. MOE Key Laboratory of Macromolecular Synthesis and Functionalization, Department of Polymer Science & Engineering, Zhejiang University, Hangzhou 310058, China; 22029005@zju.edu.cn
2. State Key Laboratory of Chemical Engineering, College of Chemical and Biological Engineering, Zhejiang University, Hangzhou 310058, China; kcao@che.zju.edu.cn
* Correspondence: wangq@zju.edu.cn

Abstract: Exploring new polymerization strategies for currently available monomers is a challenge in polymer science. Herein, a bifunctional initiator (BFI) is introduced for the conventional radical polymerization of a vinyl monomer, resulting in linear radical additions-coupling polymerization (LRAsCP). In LRAsCP, the coupling reaction alongside the addition reaction of the radicals contributes to the construction of polymer chains, which leads to stepwise growth of the multiblock structure. Theoretical analysis of LRAsCP predicted variation of some structural parameters of the resulting multiblock polymer (MBP) with the extent of initiation of the BFI and the termination factor of the radicals. Simultaneous and cascade initiations of the BFI were compared. LRAsCP of styrene was conducted, and a kinetics study was carried out. The increment in M_n with polymerization time demonstrated the stepwise mechanism of the formation of the MBP. The variation of the structural parameters of MBP fitted well with the theoretical prediction. Two-step LRAsCP was conducted and multiblock copolymers (MBcP) were obtained either by in situ copolymerization of styrene and MMA or by a second copolymerization of styrene and BMA. The current results demonstrate that the introduction of a BFI to conventional radical polymerization generates a new polymerization strategy, leading to a new chain architecture, which can be extended to other radical polymerizable monomers.

Keywords: linear radical additions-coupling polymerization (LRAsCP); kinetics analysis; bifunctional initiator; multiblock (co)polymer

1. Introduction

Multiblock polymer (MBP) has extensive applications in various fields [1–5]. Currently, its synthesis strategy includes three approaches. One is the construction of the polymer chain 'block by block' via sequential living polymerization [6–11] (Scheme 1A(1)), such as anionic polymerization [12,13], controlled radical polymerization [8,9,14–21] and olefin metathesis polymerization [10]. Although well-defined MBPs can be prepared under critical polymerization conditions with multiple steps, the tolerance of anionic polymerization limits its application in monomers with active groups, such as carboxyl and hydroxyl groups. While controlled radical polymerization can be applied to more types of monomers, the low polymerization rate implies that achieving the designed conversion and the molar mass of the polymer requires a long time to reach the designed conversion and molar mass of the polymer. The second approach is the coupling of α, ω-telechelic polymers prepared by living polymerization, which needs more than two steps (Scheme 1A(2)) [22–27]. Due to the relatively low activity of the terminal group of macromolecules, the efficiency of

the coupling reaction is unsatisfactory. The third approach is the combination of different polymerization mechanisms, which meets the same problems existing in individual methods. Exploring simple and easy methods for building polymers with complex segmental structures is still a challenge in polymer synthesis.

A. Synthetic strategies for MBP

(1) 'Block by block' involving living polymerization

(2) Coupling of

(3) This work: linear radical additions-coupling polymerization (LRAsCP)

B. Radical coupling reaction in polymerization

(1) Direct coupling of biradical/polyradical

(2) Addition-coupling of biradical/polyradical to non-homopolymerizable double bond

Multiblock Polymer (MBP)

Scheme 1. Different synthesis strategies for multiblock polymers (MBP) (**A**) and application of a radical coupling reaction in polymerization (**B**).

Radical coupling reactions are rapid reactions that have been applied in some polymerizations as a tool for building carbon–carbon bonds. Direct coupling of biradicals generates linear polymer chains (Scheme 1B(1)) [28–32]. The reaction between biradicals and various non-homopolymerized double bonds results in multi-segmental or multiblock linear polymers (Scheme 1B(2)) [22–25,33–37]. When biradicals or polyradicals are involved in radical polymerization of vinyl monomers, the radical coupling reaction is a chain extension step instead of a termination step. Radical polymerization of monovinyl monomers initiated by a polyfunctional initiator (PFI) leads to the formation of a branched polymer or polymer network. This strategy is termed non-linear radical additions-coupling polymerization (NLRAsCP) [38], in which the PFI is the source of the branching. The mechanism of NLRAsCP demonstrates that gelation is determined by the extent of initiation of the functional groups of the initiator (q) and the coupling factor of the macroradical (ϕ).

Radical polymerization is one of the oldest polymerization methods and tolerates various functional groups. It can be anticipated that when a bifunctional initiator (BFI) is introduced in the polymerization of monovinyl monomers, the coupling reaction along with the addition reaction of the radical contributes to the construction of polymer chains, producing a linear polymer composed of a multiblock structure if chain transfer to the polymer is absent. This polymerization is termed linear radical additions-coupling polymerization (LRAsCP, Scheme 1A(3)).

In this paper, we propose an efficient protocol to construct a multiblock structure via one-step LRAsCP, and two different blocks via two-step LRAsCP. The kinetic analysis of LRAsCP and its application in the synthesis of MBP and multiblock copolymers (MBcP) are investigated. Moreover, LRAsCP provides a simple approach for determining the contribution of the coupling reaction to the termination step in radical polymerization.

2. Theoretical Analysis of LRAsCP

2.1. General Process of LRAsCP

The process of LRAsCP is shown in Scheme 2. It includes three steps, such as initiation, propagation and coupling/termination, similar to normal radical polymerization. In the initiation step, the carbon radicals are formed by radical transfer reaction between bromides and pentacarbonyl manganese radical ($Mn(CO)_5\bullet$), which is generated by homolysis photolysis of decacarbonyl dimanganese ($Mn_2(CO)_{10}$) under visible light (see

Scheme S1) [39–41]. I_1XI_2, the BFI, generates three kinds of small radicals, such as $I_2XI_1\bullet$, $I_1XI_2\bullet$ and $\bullet I_1XI_2\bullet$. The first two radicals are monoradical, and the third one is biradical. In the propagation step, the three small radicals generate three macroradicals through the radical addition reaction with monomer A, such as $I_2XA_j\bullet$, $I_1XA_j\bullet$ and $\bullet A_kXA_j\bullet$. The number of macroradicals is the same as that of the corresponding small radicals. In the coupling/termination step, the radical coupling reaction between two radicals is a chain extension step instead of the termination step in conventional radical polymerization initiated by monoradical. Other reactions, such as disproportionation and chain transfer reaction, are termination steps which result in a dead end of unit A. If radicals are considered as functional groups, the coupling reaction between the macroradicals is a kind of linear coupling polymerization.
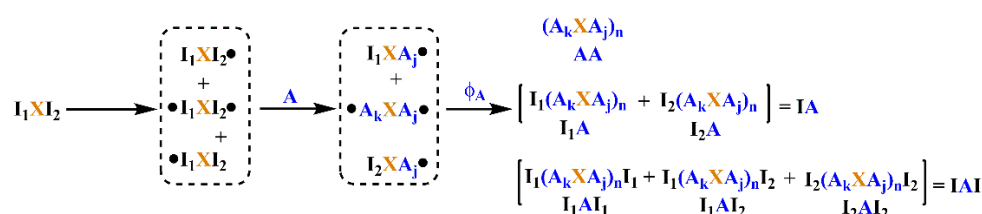
Scheme 2. LRAsCP initiated by bifunctional initiator (BFI) I_1XI_2.

Let q_1 and q_2 be the extent of initiation of groups I_1 and I_2 of BFI, and q be the total extent of initiation of BFI; then, q is equal to $0.5(q_1 + q_2)$. Let ϕ_A be the termination factor involving radical A, which is the ratio of the rate of radical coupling reaction to the overall rate of reaction consuming radicals [38]. Let δ_{11}, δ_{12}, δ_2 and δ_0 be the molar fraction of small radicals $I_2XI_1\bullet$, $I_1XI_2\bullet$, $\bullet I_1XI_2\bullet$ and free BFI, respectively. The macroradicals, $I_2XA_j\bullet$, $I_1XA_j\bullet$ and $\bullet A_kXA_j\bullet$, are formed via the radical addition reaction of the corresponding small radicals to monomer A. Their molar fractions are equal to δ_{11}, δ_{12} and δ_2, in terms of molecule, respectively. With respect to radicals, the molar fractions of the three macroradicals are represented by θ_{11}, θ_{12} and θ_2. The parameters of the δ- and θ-series can be represented by q_1 and q_2, which are summarized in Table 1.

Table 1. Various radicals formed in LRAsCP and their molar fractions.

Parameters	Monoradical		Biradical	Nonradical	Sum
	$(I_2XI_1\bullet)$	$(I_1XI_2\bullet)$	$(\bullet I_1XI_2\bullet)$	(I_2XI_1)	
Number of molecule	$\overline{q_2}q_1$	$\overline{q_1}q_2$	q_1q_2	$\overline{q_1q_2}$	1
Fraction of molecule	$\delta_{11} = \overline{q_2}q_1$	$\delta_{12} = \overline{q_1}q_2$	$\delta_2 = q_1q_2$	$\delta_0 = \overline{q_1q_2}$	1
Number of radical	$q_1\overline{q_2}$	$q_2\overline{q_1}$	$2q_1q_2$	0	$(q_1 + q_2)$
Fraction of radical	$\theta_{11} = \frac{q_1\overline{q_2}}{q_1+q_2}$	$\theta_{12} = \frac{q_2\overline{q_1}}{q_1+q_2}$	$\theta_2 = \frac{2q_1q_2}{q_1+q_2}$	0	1

Let the initial number of BFI be unity, $\overline{q_1} = 1 - q_1$, $\overline{q_2} = 1 - q_2$, $\overline{\phi_A} = 1 - \phi_A$.

The coupling reaction between three macroradicals generates six MBPs, which can be categorized into three types according to their terminal groups shown in Scheme 2. The first type is a polymer with two terminal units A, denoted as AA. The second type is a polymer with one functional group I_1 or I_2 and one terminal unit A, denoted as I_1A or I_2A. Both are collectively denoted as IA. The third type is a polymer with two functional groups, I_1 or I_2, denoted as I_1AI_1, I_1AI_2 and I_2AI_2. All three are collectively denoted as IAI.

2.2. The Number-Distribution Functions of MBP

To discuss the kinetics of LRAsCP, the following assumptions should be accepted. (1) The reactivity of all radicals is equivalent. (2) The intramolecular cycling reaction is

ignored. (3) The contribution of additional monoradical generated by chain transfer is neglected. Based on the above assumptions, the number-distribution functions ($p_{\text{MBP},n}$) of the six MBPs are given by

$$p_{\text{AA},n} = \delta_2(\theta_2\phi_\text{A})^{n-1}\overline{\phi_\text{A}}^2 = q_1q_2\overline{\phi_\text{A}}^2\left(\frac{2q_1q_2}{q_1+q_2}\phi_\text{A}\right)^{n-1} \qquad (n \geq 1) \qquad (1)$$

$$p_{\text{I}_1\text{A},n} = \delta_{12}(\theta_2\phi_\text{A})^{n-1}\overline{\phi_\text{A}} = \overline{q_1}q_2\overline{\phi_\text{A}}\left(\frac{2q_1q_2}{q_1+q_2}\phi_\text{A}\right)^{n-1} \qquad (n \geq 1) \qquad (2)$$

$$p_{\text{I}_2\text{A},n} = \delta_{11}(\theta_2\phi_\text{A})^{n-1}\overline{\phi_\text{A}} = \overline{q_2}q_1\overline{\phi_\text{A}}\left(\frac{2q_1q_2}{q_1+q_2}\phi_\text{A}\right)^{n-1} \qquad (n \geq 1) \qquad (3)$$

$$p_{\text{I}_1\text{AI}_1,n} = 0.5\delta_{12}(\theta_2\phi_\text{A})^{n-2}\theta_{12}\phi_\text{A} = 0.5\frac{(q_2\overline{q_1})^2}{q_1+q_2}\phi_\text{A}\left(\frac{2q_1q_2}{q_1+q_2}\phi_\text{A}\right)^{n-2} \qquad (n \geq 2) \qquad (4)$$

$$p_{\text{I}_1\text{AI}_2,n} = \delta_{12}(\theta_2\phi_\text{A})^{n-2}\theta_{11}\phi_\text{A} = \frac{q_1q_2\overline{q_1q_2}}{q_1+q_2}\phi_\text{A}\left(\frac{2q_1q_2}{q_1+q_2}\phi_\text{A}\right)^{n-2} \qquad (n \geq 2) \qquad (5)$$

$$p_{\text{I}_2\text{AI}_2,n} = 0.5\delta_{11}(\theta_2\phi_\text{A})^{n-2}\theta_{11}\phi_\text{A} = 0.5\frac{(q_1\overline{q_2})^2}{q_1+q_2}\phi_\text{A}\left(\frac{2q_1q_2}{q_1+q_2}\phi_\text{A}\right)^{n-2} \qquad (n \geq 2) \qquad (6)$$

where n is the number of BFI or X (residual moiety of BFI).

For example, the coupling reaction of n biradical $\bullet\text{A}_\text{k}\text{XA}_\text{j}\bullet$ results in the formation of AA-type of MBP containing n X units. The formation of this chain starts with one $\bullet\text{A}_\text{k}\text{XA}_\text{j}\bullet$, followed by $(n-1)$ coupling reactions of the same biradical and two non-coupling reactions of two terminal radicals. The corresponding probabilities for the three steps are δ_2, $(\theta_2\phi_\text{A})^{n-1}$ and $\overline{\phi_\text{A}}^2$. The product of the three probabilities yields Equation (1). The formation of I_1AI_2-type MBP starts with an $\text{I}_1\text{XI}_2\bullet$ radical, followed by coupling reaction with $(n-2)$ $\bullet\text{A}_\text{k}\text{XA}_\text{j}\bullet$ biradicals and an $\text{I}_2\text{XA}_\text{j}\bullet$ radical. The product of the corresponding probabilities, δ_{12}, $(\theta_2\phi_A)^{n-2}$ and $\theta_{11}\phi_\text{A}$, yields Equation (5). Other distribution functions can be derived by the same method and are given in Equations (1)–(6). The factor of 0.5 in Equations (4)–(6) is due to the symmetry of I_1AI_1- and I_2AI_2-type MBPs. The theoretical analysis of kinetics is described in the Supplementary Materials (SM) in detail. According to Equations (1)–(6), the distribution functions depend on q, ϕ_A and n.

2.3. The Structural Parameters of MBP

The structural parameters of MBP can be calculated from its number-distribution functions shown in Equations (1)–(6), such as the number and the fraction of each MBP (N and F) and its number-average degree of polymerization (DP_n) in terms of X. N, DP_n, the number-average molar mass (M_n) and the average number of blocks per MBP (N_K) of total MBPs can be obtained as well. Except M_n, all structural parameters of MBP are determined by three factors, q_1, q_2 and ϕ.

When more than one kind of monomer participate in LRAsCP, multiblock copolymer (MBcP) can be obtained, which is termed linear radical additions-coupling copolymerization (LRAsCcP). On the other side, at the polymerization time when the extent of initiation of I_1 and I_2 are q_{10} and q_{20}, the addition of monomer B to the polymerization mixture leads to the second-step polymerization resulting in copolymer block. Two-step LRAsCP generates two different blocks. The structural parameters of MBcP can be derived from its number-distribution function as well, which is described in the SM in detail.

3. Discussion on Theoretical Predictions of LRAsCP

Based on the mechanism of LRAsCP, the multiblock structure is predicted to be formed during the polymerization. We briefly discuss some important aspects of LRAsCP of typical

monomers, such as styrene and methyl methacrylate (MMA) with ϕ_A values of 0.93 and 0.33 [38].

3.1. Numbers and Fractions of MBPs (N_{MBP} and F_{MBP})

$$N_{AA} = q_1 q_2 \overline{\phi_A}^2 \frac{q_1 + q_2}{q_1 + q_2 - 2q_1 q_2 \phi_A} \tag{7}$$

$$N_{IA} = N_{I_1 A} + N_{I_2 A} = \frac{(q_1 + q_2)(q_1 + q_2 - 2q_1 q_2)\overline{\phi_A}}{q_1 + q_2 - 2q_1 q_2 \phi_A} \tag{8}$$

$$N_{IAI} = N_{I_1 A I_1} + N_{I_1 A I_2} + N_{I_2 A I_2} = \frac{0.5 \phi_A (q_1 + q_2 - 2q_1 q_2)^2}{q_1 + q_2 - 2q_1 q_2 \phi_A} \tag{9}$$

$$N_{P_A} = N_{AA} + N_{IA} + N_{IAI} = (q_1 + q_2)(1 - 0.5\phi_A) - q_1 q_2 \tag{10}$$

The numbers of MBPs (N) can be calculated by Equations (7)–(10) assuming the initial number of BFI (X_0) is unity, which suggests that N depends on q_1, q_2 and ϕ_A. Taking ϕ_A = 0.93 [38] as an example, the variation tendency of N is shown in Figure 1. The number of AA-type MBP (N_{AA}) monotonically increases with both q_1 and q_2 and increases rapidly as q is close to unity. (Figure 1A) The number of IA-type MBP (N_{IA}) quickly increases with both q_1 and q_2 at the beginning of polymerization. (Figure 1B) After it reaches the maximum, it rapidly decreases to null upon complete initiation. The number of IAI-type MBP (N_{IAI}) increases with q and decreases after it reaches the maximum. (Figure 1C) Moreover, its variation depends on the relative activity of the two functional groups of BFI. When the activities of I_1 and I_2 are equal ($q_1 = q_2 = q$), the case is termed simultaneous-initiation (*s*-initiation). When the activities of the two groups are remarkably different and the reactivity of I_1 is much higher than I_2, the case is termed cascade-initiation (*c*-initiation). Two special cases are shown in each figure by black and red lines, respectively. As shown by the black line in Figure 1C, N_{IAI} derived from *s*-initiation case is lower than other cases ($q_1 \neq q_2$). As shown by the red line in Figure 1C, N_{IAI} derived from *c*-initiation case is larger than other cases. The variation tendency of the number of total MBPs (N_{P_A}) shown in Figure 1D is similar to that of N_{IAI}.

$$F_{AA} = \frac{N_{AA}}{N_{P_A}} = \frac{(q_1 + q_2)q_1 q_2 \overline{\phi_A}^2}{(q_1 + q_2 - 2q_1 q_2 \phi_A)((q_1 + q_2)(1 - 0.5\phi_A) - q_1 q_2)} \tag{11}$$

$$F_{IA} = \frac{N_{IA}}{N_{P_A}} = \frac{(q_1 + q_2)(q_1 + q_2 - 2q_1 q_2)\overline{\phi_A}}{(q_1 + q_2 - 2q_1 q_2 \phi_A)((q_1 + q_2)(1 - 0.5\phi_A) - q_1 q_2)} \tag{12}$$

$$F_{IAI} = \frac{N_{IAI}}{N_{P_A}} = \frac{0.5 \phi_A (q_1 + q_2 - 2q_1 q_2)^2}{(q_1 + q_2 - 2q_1 q_2 \phi_A)((q_1 + q_2)(1 - 0.5\phi_A) - q_1 q_2)} \tag{13}$$
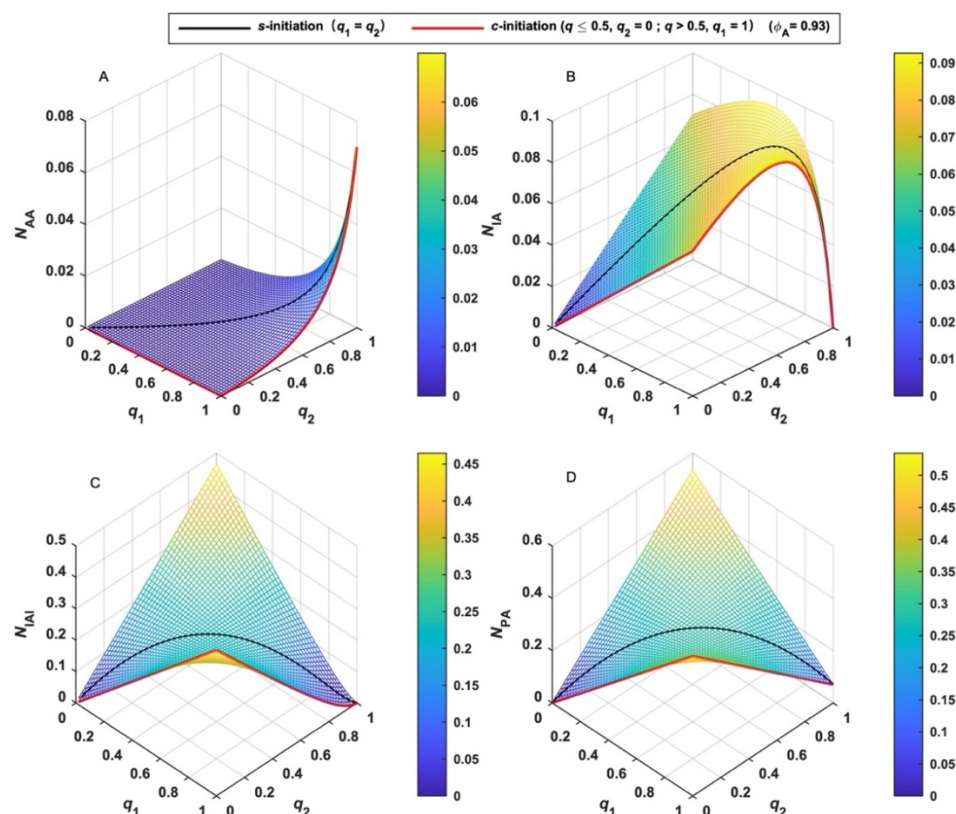
Figure 1. Variation of the number (N) of various MBPs and their sum with the extent of initiation (q) (black line for s-initiation; red line for c-initiation). (**A**): AA-type MBP; (**B**): IA-type MBP; (**C**): IAI-type MBP; (**D**): total MBPs.

The molar fractions (F) of three MBPs are given by Equations (11)–(13), and their variation tendency is shown in Figure 2. Two typical cases, such as $\phi_A = 0.93$ for styrene and 0.33 for MMA [38], were compared. It can be found in Figure 2A1 and A2 that the molar fraction of AA-type MBP (F_{AA}) is very low at the beginning of polymerization and increases gradually with q for both cases. When q is close to unity, F_{AA} increases rapidly. As shown in Figure 2C1 and C2, the variation tendency of molar fraction of IAI-type of MBP (F_{IAI}) is opposite to F_{AA} for both cases. The difference between the two cases is F_{IAI} for styrene is much higher than that of MMA, which is due to the larger ϕ. The molar fraction of IA-type MBP (F_{IA}) for styrene increases with q and reaches the maximum before the end of the initiation. (Figure 2B1) After it reaches the maximum, it decreases to null upon complete initiation. For MMA, F_{IA} decreases with q and reaches null upon complete initiation. (Figure 2B2) The difference between the two cases is mainly due to the different values of ϕ.
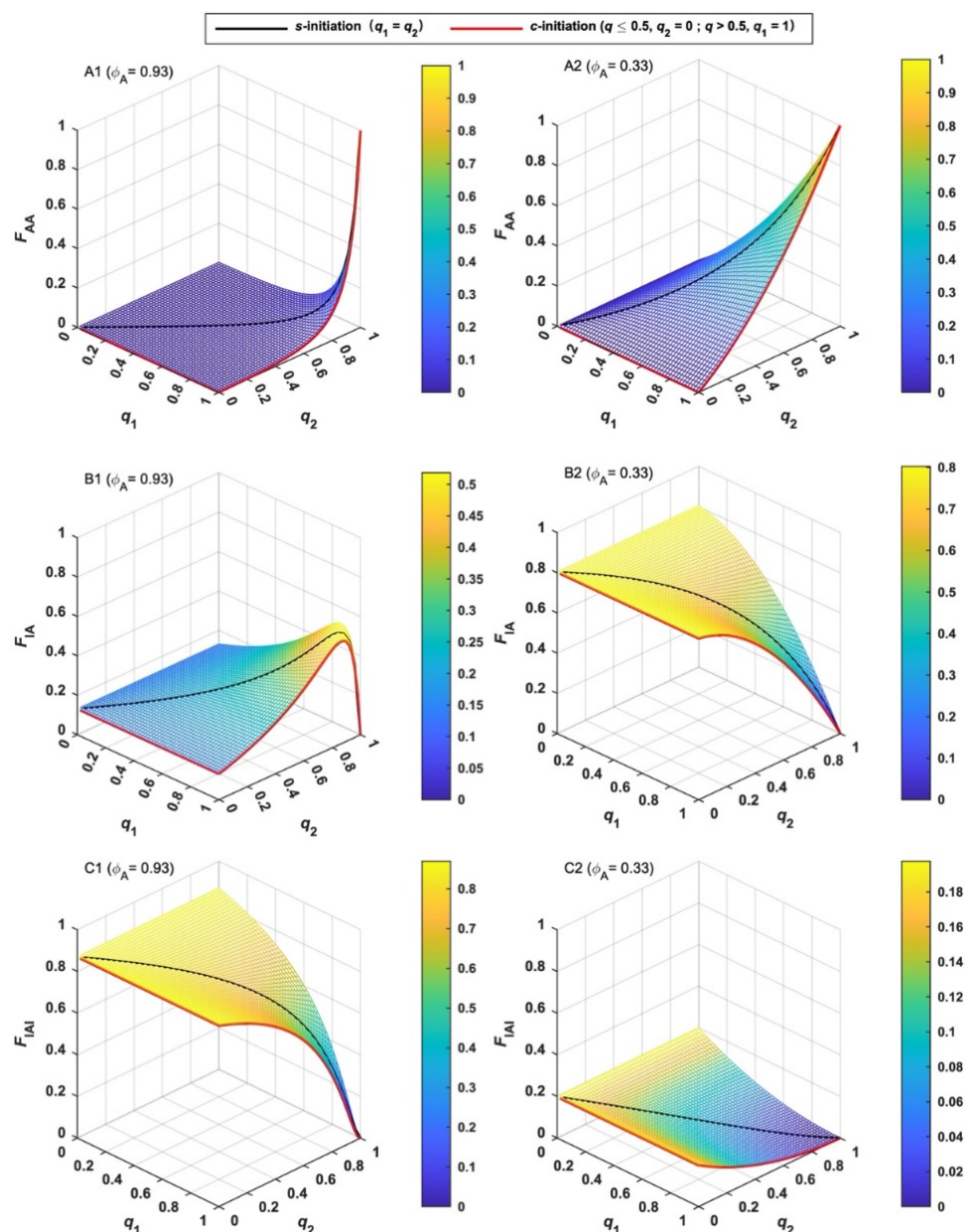
Figure 2. Variation of the molar fraction (*F*) of various MBPs with the extent of initiation (*q*) and the different coupling factors (ϕ_A). $\phi_A = 0.93$ for (**A1**, **B1** and **C1**); $\phi_A = 0.33$ for (**A2**, **B2** and **C2**).

3.2. The Number-Average Degree of Polymerization in Terms of X (DP_n)

$$DP_{n,AA} = DP_{n,IA} = \frac{q_1 + q_2}{q_1 + q_2 - 2q_1q_2\phi_A} \tag{14}$$

$$DP_{n,IAI} = 2\frac{q_1 + q_2 - q_1q_2\phi_A}{q_1 + q_2 - 2q_1q_2\phi_A} = DP_{n,IA} + 1 \tag{15}$$

$$DP_n = \frac{q_1 + q_2 - q_1q_2}{(q_1 + q_2)(1 - 0.5\phi_A) - q_1q_2} \tag{16}$$

The chain length of various MBPs formed in LRAsCP can be quantitatively evaluated by the incorporated residual BFI (X). DP_n in terms of X of various MBPs and their sum can be calculated by Equations (14)–(16), and the variation tendency with *q* is shown in Figure 3. It can be concluded that DP_n increases with both q_1 and q_2 and increases rapidly when both q_1 and q_2 approach unity. This tendency is similar to the dependence of the

degree of polymerization on polymerization time or the extent of reaction in stepwise polymerization [42]. When q exceeds 0.5 or both functional groups are initiated, the DP_n of total MBPs gradually increases, and rapidly increases when q is close to unity. The variation tendency of DP_n suggests that LRAsCP follows the stepwise mechanism since the coupling reaction is the key step in the construction of the multiblock architecture.
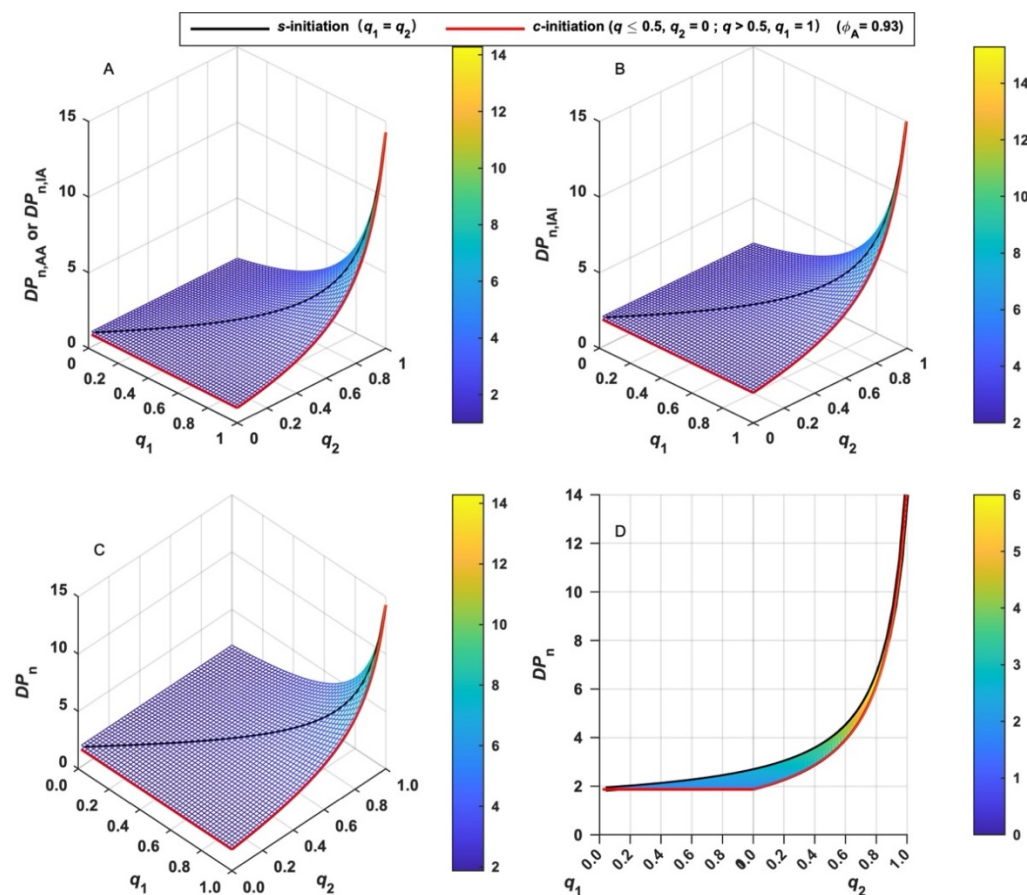

Figure 3. Variation of the number-average degree of polymerization (DP_n) of various MBPs with the extent of initiation (q). (**A**): AA- and IA-type MBP; (**B**): IAI-type MBP; (**C**): total MBPs; (**D**): total MBPs in s-initiation and c-initiation cases.

When *s*-initiation and *c*-initiation cases are compared, the difference of DP_n can be found when q is less than 0.5. As shown in Figure 3D, DP_n increases gradually with q and increases rapidly when q is close to unity for *s*-initiation case (black line), while it remains constant when q is less than 0.5 or $q_2 = 0$ for *c*-initiation case (red line). This is due to the selective initiation of one functional group of BFIs and the formation of monoradical in the early stage of *c*-initiation case ($q < 0.5$), which is the same as radical polymerization initiated by monofunctional initiator (MFI). q exceeds 0.5 when the second functional group of each BFI is initiated. Initiation of two functional groups results in the continuous formation of MBPs and an increment of DP_n in *c*-initiation case.

3.3. The Number-Average Molar Mass of Total MBPs (M_n)

Based on the number of all MBPs (N_{P_A}), the monomer conversion (C) and the number-average molar mass of total MBPs (M_n) can be calculated by Equation (17).

$$M_n = \frac{A_0 C m_A}{((q_1 + q_2)(1 - 0.5\phi_A) - q_1 q_2)X_0} \tag{17}$$

where A_0, X_0, C, and m_A are the initial concentration of monomer A and BFI, the monomer conversion and the molar mass of monomer, respectively. Since the M_n of MBP is determined by the feed ratio and the monomer conversion in addition to q_1, q_2 and ϕ_A, the discussion will be given in experimental studies.

3.4. The Average Number of Blocks per MBP (N_K)

The average number of blocks per MBP (N_K) can be evaluated by the total number of blocks and N_{P_A}, which is given by Equation (18).

$$N_K = \frac{(q_1 + q_2)(1 - 0.5\phi_A)}{(q_1 + q_2)(1 - 0.5\phi_A) - q_1 q_2} \tag{18}$$

This parameter can be experimentally evaluated and will be further discussed in experimental studies.

3.5. The Second-Step Polymerization
3.5.1. Free BFI and AA-Type MBP

$$F_{BFI} = \delta_0 = (1 - q_1)(1 - q_2) \tag{19}$$

$$W_{AA} = q_1 q_2 \overline{\phi_A}^2 \left(\frac{q_1 + q_2}{q_1 + q_2 - 2q_1 q_2 \phi_A} \right)^2 \tag{20}$$

The molar fractions of free BFI and AA-type MBP are two parameters that need to be considered if the second LRAsCP of monomer B is conducted. Free BFI might generate BB-type MBP in the second polymerization, while AA-type MBP will not initiate the second polymerization of monomer B and cannot be incorporated into MBcP. Both AA- and BB-type MBPs are impurities with respect to MBcP.

The molar fraction of free BFI (F_{BFI}) is derived in Equation (19), and its variation with q is shown in Figure 4A. When the total extent of initiation (q) is fixed, F_{BFI} has the maximum value when q_1 and q_2 are equal, and the minimum value when the difference between q_1 and q_2 is the largest. For example, free BFI disappears when $q_1 = 1$ and $q_2 = 0$ or $q \geq 0.5$ for c-initiation case (red line in Figure 4A). When $q_1 = q_2 = q = 0.5$, 25% of BFI remains for s-initiation case (black line in Figure 4A). Therefore, c-initiation case has the lowest value of F_{BFI}. In other words, c-initiation case is the best choice for the two-step polymerization.
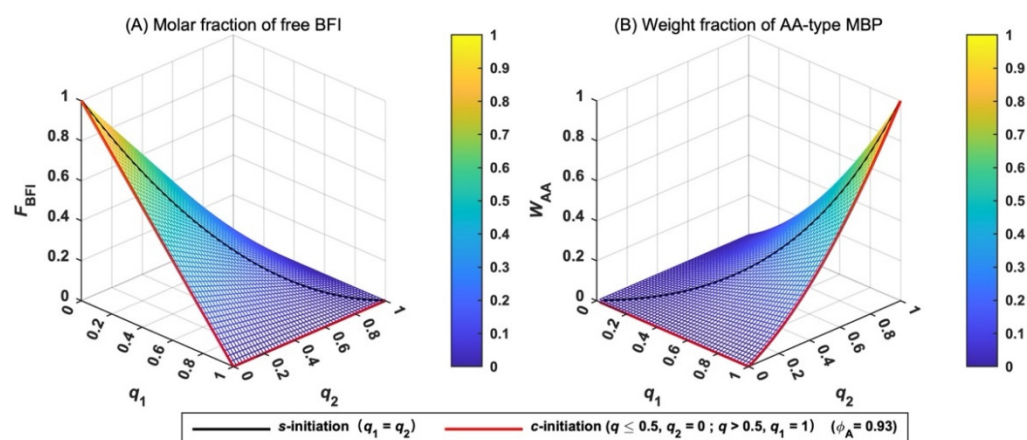

Figure 4. Variation in the molar fraction of free BFI (F_{BFI}) (**A**) and the weight fraction of AA-type MBP (W_{AA}) (**B**) with the extent of initiation (q).

The weight fraction of AA-type MBP (W_{AA}) is given by Equation (20) and its variation with q is shown in Figure 4B. When q_1 and q_2 are low, W_{AA} is small. Only when q_1 and q_2 are close to unity, W_{AA} increases rapidly. AA-type MBP formed in the first-step polymerization can be ignored in the two-step polymerization if monomer B is added when q_1 and q_2 are less than unity.

3.5.2. $DP_{n,co}$ of MBcP

$$DP_{n,co} = \frac{2}{2\overline{\phi_B} + (q_{10} + q_{20})(\phi_B - \phi_A)}$$

(21)

When monomer A is replaced by monomer B at the time when the extent of initiation is q_{10} and q_{20}, the second LRAsCP of B occurs. The $DP_{n,co}$ of total MBcP is predicted by Equation (21), assuming the complete initiation of the residual function groups of BFIs in the second polymerization. The variation tendency of $DP_{n,co}$ is shown in Figure 5. The theoretical analysis suggests that the termination factors of two monomers, ϕ_A and ϕ_B, are the key parameters affecting $DP_{n,co}$. The combination of longer polymerization of the monomer with larger ϕ and shorter polymerization of the monomer with smaller ϕ is the best way to produce MBcP with large $DP_{n,co}$. For example, when styrene is first polymerized, MMA ($\phi_B = 0.33$) is recommended to be added when q_{10} and q_{20} are close to unity. (Figure 5A) If the polymerization sequence of the two monomers is opposite, styrene is suggested to be added as early as possible (Figure 5B).
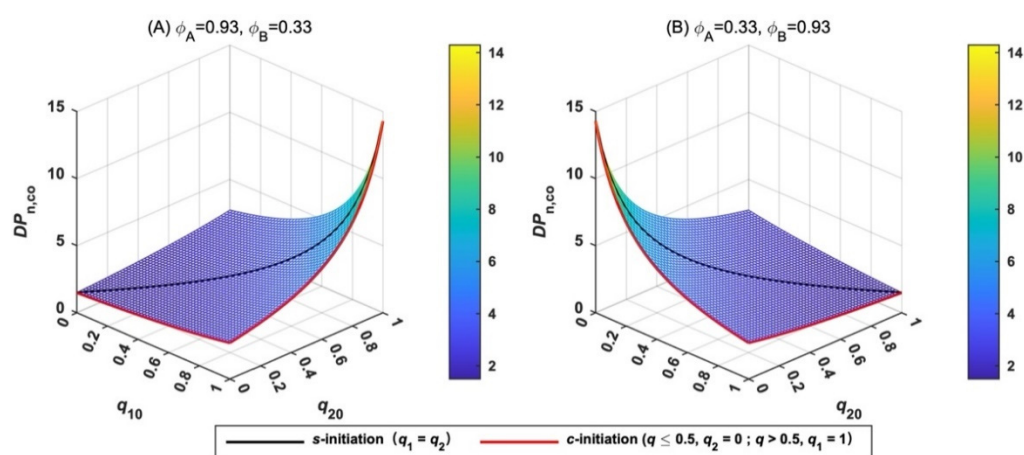

Figure 5. Variation of the degree of polymerization of the copolymerization ($DP_{n,co}$) with the extent of initiation (q_{10}, q_{20}) and the termination factors of two monomers (ϕ_A, ϕ_B). (**A**) $\phi_A = 0.93$, $\phi_B = 0.33$; (**B**) $\phi_A = 0.33$, $\phi_B = 0.93$.

In summary, the structural parameters of MBPs are determined by q and ϕ according to theoretical analysis of LRAsCP. The value of q is determined by the initiation rate and polymerization time. Φ is determined by the nature of the monomer and is the key factor to constructing the multiblock structure.

4. Experimental Study

Two initiators, I_{12} and I_2, shown in Scheme 3, were prepared from commercially available two benzylbromides I_{11} and I_1 by published methods [43]. I_{11} is a symmetrical dibromide corresponding to *s*-initiation case, and I_{12} is an unsymmetrical dibromide corresponding to *c*-initiation case.
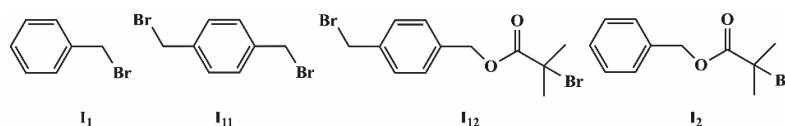
Scheme 3. The structure of initiators.

4.1. Homopolymerization of Styrene

The styrene homopolymerization initiated by I_{11} and I_{12} were conducted under the same conditions. The monomer conversion, the number-average molar mass (M_n) and its distribution of all MBPs measured by GPC are shown in Figure 6 and Tables S2 and S3.
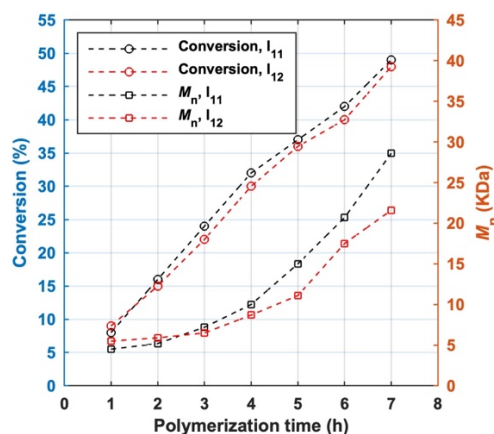

Figure 6. The variation of monomer conversion and number-average molar mass of MBP (M_n) with polymerization time.

The conversion of styrene increased with the polymerization time for both BFIs. M_n gradually increased with polymerization time before 3 h and accelerated afterwards. The variation tendency of M_n of total MBP prepared by two BFIs suggest that the coupling of macroradicals occurred in LRAsCP. Accelerated growth of M_n of total MBP after 3 h reflects the stepwise construction of the multiblock architecture. The M_n of MBPs prepared by I_{11} (*s*-initiation case) grows slightly faster than those obtained by I_{12} in the early period of polymerization, which is consistent with the tendency predicted by Equations (14)–(16) and Figure 3D. When I_{12} was used as initiator, M_n of total MBP did not remain constant at the early stage of polymerization, which suggests that LRAsCP initiated by I_{12} is not exactly *c*-initiation case, but a case between *s*-initiation and *c*-initiation. Although I_{12} is not a typical *c*-initiation case, its ester moiety introduces cleavable sites into MBPs, making the resultant MBPs degradable.

$$M_n = \frac{M_{n,0}}{q(2 - q - \phi_A)} \quad (s\text{-initiation}) \tag{22}$$

$$M_n = \begin{cases} \frac{M_{n,0}}{q(2-\phi_A)}, & q \leq 0.5 \\ \frac{M_{n,0}}{(1-q\phi_A)}, & q > 0.5 \end{cases} \quad (c\text{-initiation}) \tag{23}$$

$$M_{n,0} = \frac{A_0 C m_A}{X_0} \tag{24}$$

The M_n values of total MBP for *s*-initiation and *c*-initiation cases are further derived from Equations (17)–(22) and (23), respectively. The ratio, $A_0 C m_A / X_0$, in Equation (17) is the molar mass of polymer upon one chain per BFI, which is defined as the apparent molar mass ($M_{n,0}$) and is given by Equation (24). Since the parameters A_0, X_0, C, m_A and ϕ_A are available, the extent of initiation of the two cases at different times can be solved by Equations (22)–(24), which are given by Equations (25)–(27), respectively.

$$q = \frac{(2 - \phi_A) \pm \sqrt{(2 - \phi_A)^2 - 4R}}{2} \quad (s\text{-initiation}) \tag{25}$$

$$q = \begin{cases} \frac{R}{(2 - \phi_A)}, & q \leq 0.5 \\ \frac{1 - R}{\phi_A}, & q > 0.5 \end{cases} \quad (c\text{-initiation}) \tag{26}$$

$$M_{n,0} = \frac{A_0 C m_A}{X_0} \tag{27}$$

Based on the feed ratio, the monomer conversion and M_n of product prepared by I_{11}, the variation of q with the polymerization time estimated by Equation (25) is shown by Figure 7. It can be found that q of I_{11} for s-initiation case increased linearly with polymerization time because the polymerization is promoted by $Mn_2(CO)_{10}$/visible light. The decay of q when it was over 0.8 is due to the high monomer conversion and the gel effect observed in the polymerization [42].

$$N_K = \frac{2 - \phi_A}{2 - \phi_A - q} \quad (s\text{-initiation}) \tag{28}$$

$$N_{K,GPC} = \frac{M_n}{M_n'} \tag{29}$$
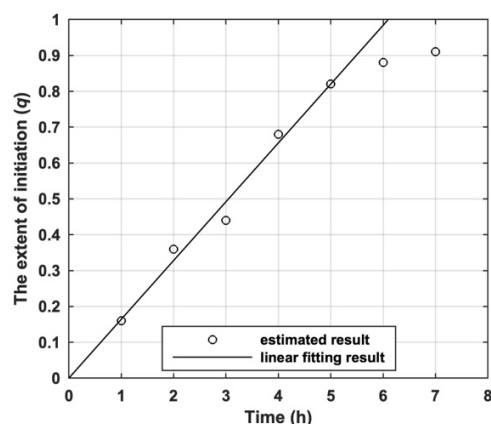
Figure 7. The variation of estimated the extent of initiation (q) of I_{11} with polymerization time.

As shown in Scheme 1 and Scheme S2, MBP is a chain composed of several segmental chains linked by moiety X. The average number of blocks per MBP (N_K) for the s-initiation case can be predicted by Equation (28) derived from Equation (18). The molar mass of the block is equal to the molar mass of the polymer generated by I_1 (M_n') in conventional radical polymerization under the same polymerization conditions if the kinetics chain length (ν) generated from two initiators are supposed to be the same. Therefore, N_K can be estimated by the ratio of M_n to M_n' measured by GPC, which is denoted as $N_{K,GPC}$ in Equation (29). As shown in Figure 8, the predicted N_K according to Equation (28) and its measured value according to Equation (29) are in good agreement.
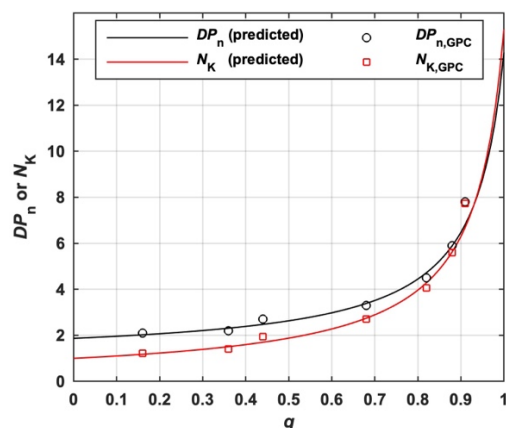
Figure 8. The variation of predicted and measured N_K and DP_n with q of I_{11} (*s*-initiation case).

On the other hand, the relationship between ν and M'_n in conventional polymerization is given by Equation (30) [42]. Therefore, ν can be quantified by the polymerization of monomer with known ϕ initiated by I_1.

$$M'_n = \frac{\nu}{1 - 0.5\phi_A} \text{ or } \nu = (1 - 0.5\phi_A)M'_n \tag{30}$$

As shown in Scheme S2, the relationship between DP_n and the number of kinetic chains per MBP (N_ν) varies with its type due to the different terminal units. If ν generated by BFI is the same as that by MFI under the same polymerization conditions, the relationship between DP_n of MBP and ν is deduced as

$$DP_{n,GPC} = \frac{M_n}{2\nu} + (0.5F_{IA} + F_{IAI}) = \frac{M_n}{(2 - \phi_A)M'_n} + (0.5F_{IA} + F_{IAI}) \tag{31}$$

$$DP_{n,GPC} = \frac{N_{K,GPC}}{(2 - \phi_A)} + \frac{1 - q}{2 - \phi_A - q} \text{ (}s\text{-initiation)} \tag{32}$$

$$DP_n = \frac{2 - q}{2 - \phi_A - q} \text{ (}s\text{-initiation)} \tag{33}$$

Equation (31) can be used to experimentally estimate the DP_n of MBP based on M_n, M'_n, F_{IA} and F_{IAI}, which is denoted as $DP_{n,GPC}$. For the *s*-initiation case, Equation (31) is reduced to Equation (32) and Equation (16) is reduced to Equation (33). $DP_{n,GPC}$ of total MBP prepared by I_{11} experimentally estimated by Equation (32) at various values of q is shown in Figure 8, which fits well with DP_n predicted by Equation (33).

4.2. Two-Step LRAsCP

Two-step LRAsCP was conducted in two ways. One is one-pot polymerization via the addition of comonomer at a certain time. LRAsCP under the same polymerization condition as Run 4 in Table S2 was conducted. After 4 h, the polymerization was suspended by turning off the light and half of the polymer solution was collected and precipitated. The resultant sample was denoted as MBP-1 (M_n = 9.4 KDa, Đ = 2.0 in Figure 9 and Table S4). MMA was added to the remaining half of the solution, and the second LRAsCP started by turning on the light for an additional 190 min. Sample MBcP-1 (M_n = 34.7 KDa, Đ = 5.1 in Figure 9 and Table S4) composed of 81 mol% styrene was obtained. This is in situ two-step LRAsCP and the second LRAsCP is the copolymerization of styrene and MMA resulting in St-MMA copolymer block. The obtained MBP-1 contains both IA- and IAI-type MBPs and was used as macro-initiator for the copolymerization of styrene and butyl methacrylate (BMA) for 4 h. Sample MBcP-2 (M_n = 38.6 KDa, Đ = 5.0 in Figure 9

and Table S4) composed of 89 mol% styrene was obtained. The improved molar masses of MBcP-1 and MBcP-2 compared with that of MBP-1 demonstrates that LRAsCP continues in the second-step polymerizations in two different ways. MBcP-2 is composed of 75 wt% polystyrene block and 25 wt% styrene-BMA (49/51, mol/mol) copolymer block and the glass transition temperature (T_g) of 53 °C was detected by DSC, which is different from the T_g of PS (100 °C) and PBMA (21 °C). This confirms that a copolymer block was formed during the second-step LRAsCP.
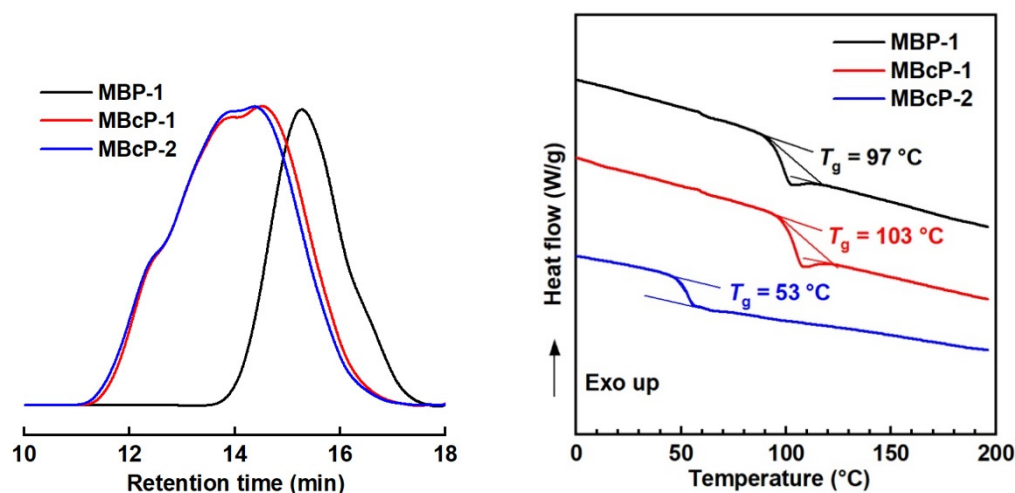
Figure 9. GPC (**left**) and DSC (**right**) curves of MBP-1, MBcP-1 and MBcP-2 prepared by I$_{11}$.

4.3. Determination of φ of Different Monomers

The termination mode in terms of $k_{t,c}/(k_{t,c} + k_{t,d})$ is a key parameter in radical polymerization kinetics. Several experimental methods, such as isotopic labeling of the initiator [44], transformation of initiator fragments after polymerization [45], gelation technique [46,47] and MALDI analysis of polymer [48], have been proposed to determine the termination mode. These methods are based on quantitative analysis of the chain end, which is still difficult because the concentration of initiator fragments is low. Since the N_K of MBP produced in LRAsCP is determined by ϕ, it is possible to acquire the value of ϕ in LRAsCP. Replacing N_K in Equation (28) with $N_{K,GPC}$ in Equation (29) yields Equation (34).

$$q = \left(1 - N_{K,GPC}^{-1}\right)(2 - \phi_A) \tag{34}$$

If the same q is achieved under the same polymerization conditions, Equation (34) can be applied to measure the factor ϕ of any polymerization based on $N_{K,GPC}$ and known ϕ of styrene. The polymerization of styrene, MMA and BMA initiated by I$_{11}$ and I$_1$ were conducted at the same conditions for 3 h and the polymerization results are given in Table S5. The number-average molar mass of the six samples prepared by I$_{11}$ (M_n) and I$_1$ (M_n') results in different $N_{K,GPC}$. With known ϕ of styrene (0.93) [38], the calculated value of ϕ of MMA is 0.33 according to Equation (34), which is the same as that determined by the measurement of gelation point in NLRAsCP of MMA [38]. The calculated ϕ of BMA is −0.25, which is obviously unreasonable. This is probably due to the gelation effect caused by the high monomer conversion and the chain transfer reaction to the polymer. Although the factor ϕ is not the same as $k_{t,c}/(k_{t,c} + k_{t,d})$, LRAsCP provides an easy method of quantitative determination of the contribution of the coupling reaction in the termination step of radical polymerization independent of the initiator fragment.

5. Conclusions

LRAsCP initiated by BFI and its kinetics modal have been proposed. Theoretical analysis of LRAsCP provides the quantitative relationships between some key parameters of MBP, such as the molar fraction of various MBPs, DP_n, M_n, N_K with q and ϕ. The s-initiation case of LRAsCP of styrene initiated by $\mathbf{I_{11}}$/Mn$_2$(CO)$_{10}$/visible light were intensively investigated. The experimental results fit well with the theoretical predictions, which approve the stepwise construction of the multiblock structure of MBP. MBcP composed of two types of blocks, PS block and P(St-MMA/BMA) block, can be produced by two-step LRAsCP. Furthermore, LRAsCP can be applied to the measurement of ϕ of radicals when ϕ of one specific monomer is known. The current results demonstrate that the introduction of BFI to conventional radical polymerization generates a new polymerization strategy, which is a facile method to construct the multiblock structure. Since radical polymerization is tolerant to various monomers, LRAsCP can be extended to other monomers that are difficult to be polymerized by living and controlled radical polymerizations.

6. Experimental Section

Two initiators, I$_2$ and I$_{12}$, shown in Scheme 2 were prepared by the reaction between I$_1$ or I$_{11}$ and 2-bromoisobutanoic acid by published methods [43]. The structure of two compounds was confirmed by NMR, HRMS. The homopolymerization of styrene and copolymerization of styrene with MMA and BMA promoted by Mn$_2$(CO)$_{10}$/visible light were conducted. MBPs were characterized by GPC, and MBcPs were characterized by GPC and NMR. Full descriptions of the methods and analytical data for the compounds and polymer used and generated in the study are given in the Supplementary Materials.

Abbreviations

Abbreviation/symbol	Definition
A, A_0	the concentration and initial concentration of monomer
B(M)FI	bi(mono)functional initiator
MB(c)P	multiblock (co)polymer
C	the conversion of monomer
f	the functionality of MBP
F_{AA}, F_{IA}, F_{IAI}	the molar fraction of three types of MBPs
M_n	the number-average molar mass of MBP prepared by BFI
$M_{n,0}$	the apparent number-average molar mass
m_A	the molar mass of monomer A
N_{AA}, N_{IA}, N_{IAI}	the number of three types of MBPs
N_K	the average number of blocks per MBP
$N_{K,GPC}$	the average number of blocks per MBP estimated by GPC
N_{P_A}	the total number of MBPs
N_v	the number of kinetic chains per MBP
$p_{AA,n}$, $p_{I_1A,n}$, $p_{I_1AI_2,n}$	the number-distribution functions of different kinds of MBPs
q	the extent of initiation of functional group
W	the weight fraction of MBP
X, X_0	residual fragment of BFI, the concentration and initial concentration of BFI
DP_n	the number-average degree of polymerization in terms of X
$DP_{n,GPC}$	DP_n estimated by molar mass of MBP (GPC)
$DP_{n,co}$	DP_n of MBcP
δ	the molar fraction of small radicals
θ	the molar fractions of macroradicals
ϕ	termination factor
ν	kinetic chain length

References

1. Qiang, X.; Chakroun, R.; Janoszka, N.; Groeschel, A.H. Self-Assembly of Multiblock Copolymers. *Isr. J. Chem.* **2019**, *59*, 945–958. [CrossRef]
2. Steube, M.; Johann, T.; Barent, R.D.; Mueller, A.H.E.; Frey, H. Rational design of tapered multiblock copolymers for thermoplastic elastomers. *Prog. Polym. Sci.* **2022**, *124*, 101488. [CrossRef]
3. Luo, Y.; Guo, Y.; Gao, X.; Li, B.-G.; Xie, T. A General Approach Towards Thermoplastic Multishape-Memory Polymers via Sequence Structure Design. *Adv. Mater.* **2013**, *25*, 743–748. [CrossRef]
4. Self, J.L.; Zervoudakis, A.J.; Peng, X.; Lenart, W.R.; Macosko, C.W.; Ellison, C.J. Linear, Graft, and Beyond: Multiblock Copolymers as Next-Generation Compatibilizers. *JACS Au* **2022**, *2*, 310–321. [CrossRef]
5. Constantinou, A.P.; Sam-Soon, N.F.; Carroll, D.R.; Georgio, T.K. Thermoresponsive Tetrablock Terpolymers: Effect of Architecture and Composition on Gelling Behavior. *Macromolecules* **2018**, *51*, 7019–7031. [CrossRef]
6. Bates, F.S.; Hillmyer, M.A.; Lodge, T.P.; Bates, C.M.; Delaney, K.T.; Fredrickson, G.H. Multiblock Polymers: Panacea or Pandora's Box? *Science* **2012**, *336*, 434–440. [CrossRef]
7. Beyer, V.P.; Kim, J.; Becer, C. R. Synthetic approaches for multiblock copolymers. *Polym. Chem.* **2020**, *11*, 1271–1291. [CrossRef]
8. Tang, X.; Fan, X.; Chen, X.; Zhou, Q. Progress of Atom Transfer Radical Polymerization (ATRP) Applied to the Synthesis of Multiblock Copolymers. *Polym. Bull.* **2006**, *6*, 36–43.
9. Clothier, G.K.K.; Guimaraes, T.R.; Thompson, S.W.; Rho, J.Y.; Perrier, S.; Moad, G.; Zetterlund, P.B. Multiblock copolymer synthesis *via* RAFT emulsion polymerization. *Chem. Soc. Rev.* **2023**, *52*, 3438–3469. [CrossRef]
10. Gringolts, M.L.; Denisova, Y.I.; Finkelshtein, E.S.; Kudryavtsev, Y.V. Olefin metathesis in multiblock copolymer synthesis. *Beil. J. Org. Chem.* **2019**, *15*, 218–235. [CrossRef]
11. Diaz, C.; Mehrkhodavandi, P. Strategies for the synthesis of block copolymers with biodegradable polyester segments. *Polym. Chem.* **2021**, *12*, 783–806. [CrossRef]
12. Steube, M.; Johann, T.; Galanos, E.; Appold, M.; Ruettiger, C.; Mezger, M.; Gallei, M.; Müller, A.H.E.; Floudas, G.; Frey, H. Isoprene/Styrene Tapered Multiblock Copolymers with up to Ten Blocks: Synthesis, Phase Behavior, Order, and Mechanical Properties. *Macromolecules* **2018**, *51*, 10246–10258. [CrossRef]

13. Gleede, T.; Rieger, E.; Blankenburg, J.; Klein, K.; Wurm, F.R. Fast Access to Amphiphilic Multiblock Architectures by the Anionic Copolymerization of Aziridines and Ethylene Oxide. *J. Am. Chem. Soc.* **2018**, *140*, 13407–13412. [CrossRef] [PubMed]

14. Tanaka, J.; Gurnani, P.; Cook, A.B.; Haekkinen, S.; Zhang, J.; Yang, J.; Kerr, A.; Haddleton, D.M.; Perrier, S.; Wilson, P. Microscale synthesis of multiblock copolymers using ultrafast RAFT polymerisation. *Polym. Chem.* **2019**, *10*, 1186–1191. [CrossRef]

15. Nishimura, S.-n.; Higashi, N.; Koga, T. Facile Synthesis of Multiblock Copolymers Containing Sequence-Controlled Peptides and Well-Defined Vinyl Polymers by Nitroxide-Mediated Polymerization. *Chem. A Eur. J.* **2017**, *23*, 15050–15058. [CrossRef]

16. Kuroki, A.; Martinez-Botella, I.; Hornung, C.H.; Martin, L.; Williams, E.G.L.; Locock, K.E.S.; Hartlieb, M.; Perrier, S. Looped flow RAFT polymerization for multiblock copolymer synthesis. *Polym. Chem.* **2017**, *8*, 3249–3254. [CrossRef]

17. Kerr, A.; Hartlieb, M.; Sanchis, J.; Smith, T.; Perrier, S. Complex multiblock bottle-brush architectures by RAFT polymerization. *Chem. Commun.* **2017**, *53*, 11901–11904. [CrossRef]

18. Engelis, N.G.; Anastasaki, A.; Nurumbetov, G.; Truong, N.P.; Nikolaou, V.; Shegiwal, A.; Whittaker, M.R.; Davis, T.P.; Haddleton, D.M. Sequence-controlled methacrylic multiblock copolymers via sulfur-free RAFT emulsion polymerization. *Nat. Chem.* **2017**, *9*, 171–178. [CrossRef]

19. Anastasaki, A.; Oschmann, B.; Willenbacher, J.; Melker, A.; Van Son, M.H.C.; Truong, N.P.; Schulze, M.W.; Discekici, E.H.; McGrath, A.J.; Davis, T.P.; et al. One-Pot Synthesis of ABCDE Multiblock Copolymers with Hydrophobic, Hydrophilic, and Semi-Fluorinated Segments. *Angew. Chem. Int. Ed.* **2017**, *56*, 14483–14487. [CrossRef]

20. Aksakal, R.; Resmini, M.; Becer, C.R. Pentablock star shaped polymers in less than 90 minutes *Via* aqueous SET-LRP. *Polym. Chem.* **2016**, *7*, 171–175. [CrossRef]

21. Gody, G.; Barbey, R.; Danial, M.; Perrier, S. Ultrafast RAFT polymerization: Multiblock copolymers within minutes. *Polym. Chem.* **2015**, *6*, 1502–1511. [CrossRef]

22. Zhang, C.; Wang, Q. Degradable Multisegmented Polymers Synthesized by Consecutive Radical Addition-Coupling Reaction of alpha,omega-Macrobiradicals and Nitroso Compound. *J. Polym. Sci. Part A Polym. Chem.* **2011**, *49*, 612–618. [CrossRef]

23. Zhu, Q.; Wang, Q. Thermodegradable multisegmented polymer synthesized by consecutive radical addition-coupling reaction of α, ω-macrobiradicals and dithioester. *J. Polym. Sci. Part A Polym. Chem.* **2012**, *50*, 2029–2036. [CrossRef]

24. Tao, F.; Li, J.; Wang, Q. Aqueous radical addition-coupling polymerization for the synthesis of hydrophilic periodic polymer. *RSC Adv.* **2014**, *4*, 53253–53256. [CrossRef]

25. Tao, F.; Wang, Q. Aqueous radical addition-coupling polymerization using a nitroso benzene/cyclodextrin complex for the synthesis of a hydrophilic periodic polymer. *RSC Adv.* **2015**, *5*, 46007–46010. [CrossRef]

26. Zhu, X.; Wang, Z.; Liu, J.; Min, X.; Wang, T.; Fan, X. A New Strategy to Synthesize α,ω-Dihydroxy Multiblock Copolymers via CpRu(CH$_3$CN)$_3$ PF$_6$/Quinaldic Acid Catalyst. *Macromol. Rapid Commun.* **2019**, *40*, 1900135. [CrossRef]

27. Beyer, V.P.; Cattoz, B.; Strong, A.; Phillips, D.J.; Schwarz, A.; Becer, C. R. Fast track access to multi-block copolymers *via* thiol-bromo click reaction of telechelic dibromo polymers. *Polym. Chem.* **2019**, *10*, 4259–4270. [CrossRef]

28. Cianga, I.; Yagci, Y. First polyrecombination reaction via atom transfer radical coupling (ATRC), a new way for the synthesis of poly(p-xylylene). *Des. Monomers Polym.* **2007**, *10*, 575–584. [CrossRef]

29. Durmaz, Y.Y.; Aydogan, B.; Cianga, I.; Yagci, Y. The Use of Atom Transfer Radical Coupling Reactions for the Synthesis of Various Macromolecular Structures. *Polym. Prepr.* **2008**, *49*, 382–383.

30. Wang, C.H.; Song, Z.Y.; Deng, X.X.; Zhang, L.J.; Du, F.S.; Li, Z.C. Combination of ATRA and ATRC for the Synthesis of Periodic Vinyl Copolymers. *Macromol. Rapid Commun.* **2014**, *35*, 474–478. [CrossRef]

31. Liu, Z.; Wang, Q. Radical coupling copolymerization (RCCP) for synthesis of various polymers. *Polymer* **2016**, *100*, 56–59. [CrossRef]

32. Liu, Z.; Wang, Q. Radical coupling polymerization (RCP) for synthesis of various polymers. *RSC Adv.* **2016**, *6*, 39568–39572. [CrossRef]

33. Zhang, C.; Wang, Q. Step-Growth Radical Addition-Coupling Polymerization (RACP) for Synthesis of Alternating Copolymers. *Macromol. Rapid Commun.* **2011**, *32*, 1180–1184. [CrossRef] [PubMed]

34. Zhang, C.; Ling, J.; Wang, Q. Radical Addition-Coupling Polymerization (RACP) toward Periodic Copolymers. *Macromolecules* **2011**, *44*, 8739–8743. [CrossRef]

35. Zhang, C.; Wang, Q. Block copolymers prepared by polymeric radical addition cross-coupling reaction to different double bonds. *J. Polym. Sci. Part. A Polym. Chem.* **2013**, *51*, 2817–2823. [CrossRef]

36. Li, J.; Wang, Q. Radical Addition-Coupling Polymerization with Various Nitroso Compounds. *J. Polym. Sci. Part A Polym. Chem.* **2014**, *52*, 810–815. [CrossRef]

37. Liu, Z.; Wang, Q. Radical addition-coupling polymerization (RACP) of various benzyl-type biradical toward periodic polymers. *Polymer* **2016**, *94*, 14–18. [CrossRef]

38. Ren, L.M.; Li, C.L.; Wang, Q. Non-linear Radical Additions-Coupling Polymerization of Monovinyl Monomers towards Polymer Networks: Theory, Tunability and Heritable Architecture. *Chin. J. Polym. Sci.* **2022**, *40*, 1623–1630. [CrossRef]

39. Gilbert, B.C.; Harrison, R.J.; Lindsay, C.I.; McGrail, P.T.; Parsons, A.F.; Southward, R.; Irvine, D. J. Polymerization of methyl methacrylate using dimanganese decacarbonyl in the presence of organohalides. *Macromolecules* **2003**, *36*, 9020–9023. [CrossRef]

40. Haines, L.I.B.; PoЁ, A.J. Initiation of Vinyl Polymerization by Manganese Carbonyl and Carbon Tetrachloride. *Nature* **1967**, *215*, 699–701. [CrossRef]

41. Ciftci, M.; Tasdelen, M.A.; Yagci, Y. Sunlight induced atom transfer radical polymerization by using dimanganese decacarbonyl. *Polym. Chem.* **2014**, *5*, 600–606. [CrossRef]

42. Odian, G. *Principles of Polymerization*, 4th ed.; Wiley & Sons, Inc.: Hoboken, NJ, USA, 2004.

43. Dewkar, G.K.; Carneiro, P.B.; Hartman, M.C.T. Synthesis of Novel Peptide Linkers: Simultaneous Cyclization and Labeling. *Org. Lett.* **2009**, *11*, 4708–4711. [CrossRef] [PubMed]

44. Arnett, L.M.; Peterson, J.H. Vinyl Polymerization with Radioactive Aliphatic Azobisnitrile Initiators. *J. Am. Chem. Soc.* **1952**, *74*, 2031–2033. [CrossRef]

45. Bamford, C.H.; Jenkins, A.D. Termination Reaction in Vinyl Polymerization: Preparation of Block Copolymers. *Nature* **1955**, *176*, 78. [CrossRef]

46. Bamford, C.H.; Dyson, R.W.; Eastmond, G.C. Studies in network formation. *J. Polym. Sci. Part C Polym. Symp.* **1967**, *16*, 2425–2434. [CrossRef]

47. Bamford, C.H.; Eastmond, G.C.; Whittle, D. Network formation III—Influence of organometallic initiator on network structure. *Polymer* **1969**, *10*, 771–783. [CrossRef]

48. Zammit, M.D.; Davis, T.P.; Haddleton, D.M.; Suddaby, K.G. Evaluation of the mode of termination for a thermally initiated free-radical polymerization via matrix-assisted laser desorption ionization time-of-flight mass spectrometry. *Macromolecules* **1997**, *30*, 1915–1920. [CrossRef]